How to Cite:
l-wahid, A. A., Najim, S. S., & Rady, H. H. (2022). Removing of some heavy metals from cutting rock samples by using nano graphene oxide. *International Journal of Health Sciences*, *6*(S2), 9279–9291. https://doi.org/10.53730/ijhs.v6nS2.7429

Removing of some heavy metals from cutting rock samples by using nano graphene oxide

Ahamed Abdu l-wahid
Chemistry department, Collage of Science, Misan University, Maysan- Iraq

Safaa Sabri Najim
Chemistry department, Collage of Science, Misan University, Maysan- Iraq
Corresponding author email: safchem2000@uomisan.edu.iq

Hawraa Hameed Rady
Chemistry department, Collage of Science, Misan University, Maysan- Iraq

***Abstract*---**A modified Totland's approach was used to separate and preconcentrate trace elements from cutting rock samples obtained from different depths of oil fields in Maysan Province, Iraq. FT-IR, UV-Vis spectrophotometer, (XRD) X-ray diffraction spectroscopy, (ZP) Zeta potential analyzer, and (FESEM) field emission scanning electronic microscopy, were used to characterize (NGO) nano graphene oxide, synthesized by a modified Hummer's method. The (SPME) method solid phase micro extraction method employed to remove the trace elements (Mg, Co, Ni, Cu, Cd, and Pb) from cutting rock samples under the optimum conditions. The average concentrations of Magnesium, Cobalt, Nickel, Copper, Cadmium, and Lead, the average concentrations in cutting rock samples (direct technique) were (9.72 g/mL), (1.318 g/mL), (5.646 g/mL), (0.616 g/mL), (0.567 g/mL), and (9.296 g/mL). The average element concentrations by SPME technique (2.082 g/mL), (0.24 g/mL), (1.066 g/mL), (0.162 g/mL), (0.055 g/mL), and (2.153 g/mL) for Magnesium, Cobalt, Nickel, Copper, Cadmium, and Lead, respectively were decreased, confirming the chemical adsorption process on the (NGO) surface sheets.

***Keywords*---**trace elements, SPME, nanosheets, graphene oxide, cutting rocks, FESEM.

Introduction

Prior to the introduction of atomic absorption spectrometry, SPME is a prominent method for separating and pre-concentrating metal ions (AAS) [(1)]. In the solid phase micro extraction process, nano graphene oxide is used as a sorbent (SPME)

[2]. This material is characterized by layers with a high specific surface area and strong van der Waals interactions, hydrophobic graphene oxide sheets have been dispersed directly in water, widely regarded as an unsolvable problem. Surface-active compounds[3] as well as polar solvents as solubilizes ,dispersion agents are used to pre-concentrate analyses [4], This might lead to irreversible agglomerates or even graphite restacking, thus halting graphene oxide production[5].

Nano graphene oxide is has two-dimensional (2D) crystalline, consisting of a carbon atom monolayer with a C-C bond spacing of 0.142 nm [6] . Having a big specific surface area in theory and a high specific surface area in absorption capacity (2630 m^2g^{-1}) [7]. It's made up of carboxyl, carbonyl, hydroxyl, and epoxy functional groups in a hexagonal carbon network [8]. Nano graphene oxide is an excellent metal ion sorbent due to both electrostatic and coordinate processes since these Metal ions may be joined by oxygen-containing functional groups, especially multivalent metal ions. [9]. Nano Graphene Oxide (NGO) is a novel adsorbent carbon with brilliant features that make it an exceptional sorbent for the pre-concentration of trace metal ions, the availability of both sides of the planar sheets of graphene oxide for adsorption. Because both sides of the planar sheets of graphene oxide are available for molecule adsorption, Nano Graphene Oxide (NGO) is an unique form of carbon adsorbent with exceptional properties, because of its huge surface area, this sorbent has a high adsorption capacity and efficacy [10]. The goal of this work is to isolate trace elements from cutting rock samples from various depths of oil fields using the SPME method and synthesized NGO as a sorbent; the application is the study's originality.

Methodology

Instrumentation

Table-1 shows the operational conditions of FAAS. The analytes (Mg, Co, Ni, Cu, Cd, and Pb) were measured by using the AI-1200 Aurora flame atomic absorption spectroscopy. Shimadzu UV-1800 double beam spectrophotometer, Shimadzu X-ray diffraction (XRD, LabX-XRD-6000,) Shimadzu FTIR-8400S fourier transform infrared spectrophotometer (ELS type, zeta plus, Brookhaven).

Field emission scanning electronic microscopy (FESEM, 5KV, Zeiss), probe sonicator (FSFJY92-IIN, Sino Sonics) and stirring water bath (KBLEE 2010).

Table-1 Operational parameters of FAAS according to manufacturer's operational manual

Elements	Wave length (nm)	Slit width (nm)	HCL (mA)	Calibration range (µg/mL)	Flame
Mg	285.2	0.2	5	0.5 – 2	Air/acetylene
Co	240.7	0.2	7	0.5 – 2	Air/acetylene
Ni	232.0	0.2	7	0.5 – 2	Air/acetylene
Cu	324.7	0.2	6	0.5 – 2	Air/acetylene
Cd	288.8	0.2	5	0.5 – 2	Air/acetylene

Pb	217.0	0.2	5	2.0 – 8	Air/acetylene

Chemicals

All solutions were prepared with deionized water (19.5 S/cm), working standard solutions were prepared by diluting the stock solutions (1000 g/mL) in a series step. $MgSO_4$, $CoSO_4$, $NiSO_4$, $CuSO_4$, $CdSO_4$, $Pb(NO_3)_2$, purchased from Sigma-Aldrich. CDH firm, graphite (99.9%),Potassium permanganate, Sodium nitrate/ Thomas beaker, Sulfuric acid (97%) ChemLab, Dimethyl formamide (99.5%) Applichem (37%) hydrochloric acid, hydrogen peroxide (50 percent) Applab Panreac

Samples collection

Cutting rock samples has collected from different depths of oil reservoirs (Mishrif formation) in Maysan province south east of Iraq, Amarah oil field depth (2874-3240 m), Noor oil field depth (3301-3668 m), Halfaya oil field depth (3102-3432 m), north Buzurgan oil field depth (3698-4021 m) and south Buzurgan oil field depth (3674-4016 m), as shown in Fig. (1).

Fig.1: Oil fields in Maysan province- Iraq

Synthesis of nano graphene oxide

The GO synthesized by the Hummer's method with some modification as shown in Fig.2. The specific steps for the synthesis were as follows: First, a certain volume of concentrated H_2SO_4 (23 mL) was added to the mixture of graphite flakes (1 g) and $NaNO_3$ (0.5 g) followed by cooling to 0-5C^0 with an ice bath. Then, (3 g) $KMnO_4$ was added to the mixture slowly, the mixture warmed to 35 C^0 with magnetic stirring for 30 min. An additional amount of water (100 mL) was added slowly with magnetic stirring for another 30 min. After completing the reaction, 5 mL 30% H_2O_2 was added to the mixture, bubbles appeared from the aqueous mixture and brilliant yellow color were observed. After settling for approximately 12 h, the clear supernatant of the mixture was decanted. The precipitate was washed repeatedly with deionized water [11,12].

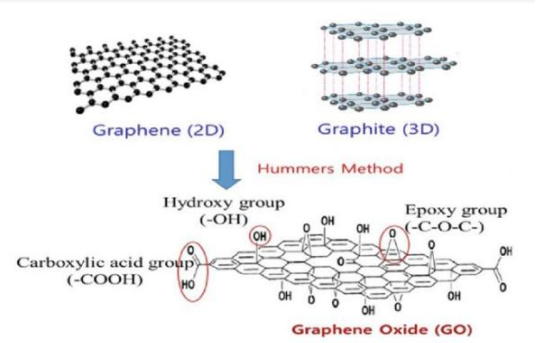

Fig.2: Synthesis of NGO

Optimum conditions of the solid phase micro extraction method (SPME)

The analyte ions in cutting rock samples were determined directly by FAAS (Mg, Co, Ni, Cu, Cd, and Pb). The optimum conditions for the (SPME) by NGO were: (20 ml) volume of digested sample, optimum pH for each analyte ions, 0.5 mg of (NGO), sonicating for (2 min), stirring for (5 min) at room temperature, centrifuged for (5 min at 5000 rpm).

Samples digestion

Each sample grinded by electrical grinder, sieved by standard sieve (0.3 mm) portion of the powder, dried by oven at 105 ºC for an hour, cool to room temperature in the desiccator. The samples digested by a modified Totland's method[13,14], weighed (0.5 g) of each sample into Teflon beaker and moistened with (3 mL) of deionized water, (10 mL) concentrated hydrofluoric acid added and (4 mL) concentrated perchloric acid. The mixture heated at 200 ºC to dryness and crystalline paste appeared after 1.5 hrs., this step is repeated one time. Concentrated perchloric acid (4 mL) added and evaporated to near dryness at 200 ºC (0.5 hrs.), 10 ml of (5M) Nitric acid added, heated gently at (65 ºC) until a clear solution appeared, cooling and diluted with deionized water up to the mark of volumetric flask (50 mL), Polypropylene containers were used to store the samples.

Results and Discussion

Nano Graphene oxide (NGO) Characterization

The FT-IR spectra of synthesized nano graphene oxide as shown in Fig. 3-a (NGO), which includes a band at 1626 cm^{-1} for the C=C bond, a broad band of the OH bond at 3360-3460 cm^{-1}, the C=O band stretching vibrations of carbonyl and carboxylic groups at around 1709 cm-1, and bands at 1217 cm^{-1} to COH and 1035 cm^{-1} to CO of epoxy group stretching vibrations at around 1709 cm^{-1}. The peak of absorption, λ_{max}= 239.5 nm, and a shoulder peak at 289.5 nm, were the absorption bands indicate to the (NGO) dispersion (0.1 mg/mL), as shown in Fig. 3-b. n-π* electron transitions of C=O bonds and π-π * electron transitions of poly aromatic C=C bonds [15]. The zeta potential of the produced NGO (-17.17 mV), as

shown in Fig. 3-c, the surface charge on NGO, which has an impact on nanomaterial aggregation and ion adsorption on the nano surface sheets. [16] The XRD spectrum in Fig. 3-d, the peak 2θ = 26.7° [17], to the oxidation process for graphite, new peak appeared at (2θ ≈11°) indicating the presence of the NGO, the findings are consistent with earlier research. [18,19] The FESEM used to study the corrugation form noticed on the surface morphology of (NGO) as depicted in Fig. 3. Low wrinkled (GO) surface nano sheets are more sensitive and have superior adsorption ability [20]. As shown in Fig. 4, The energy dispersive X-ray (EDX) (attached to the FESEM) was used to identify the elements involved in the formation of nano sheets of (GO), with a peak for carbon atoms at energy (0.18 keV) and another peak for oxygen atoms at energy (0.5 keV) proving the presence of carbon and oxygen atoms only in pure synthesized NGO. The findings are very similar to those obtained in previous studies [21, 22].

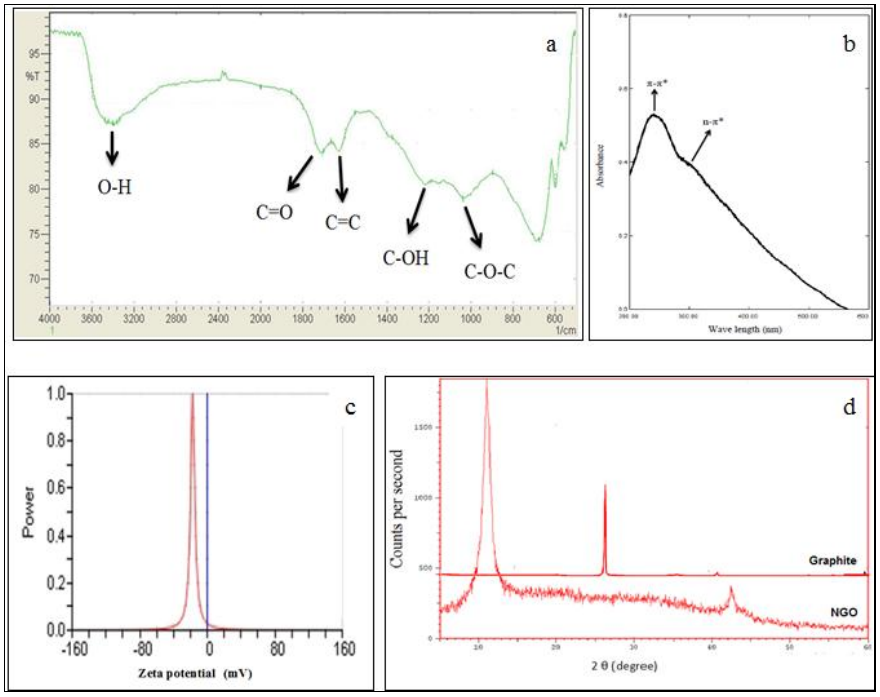

Fig.-3: Characterization of synthesized NGO (a) FT-IR, (b) UV-vis absorption spectrum, (c) Zeta potential, (d) XRD

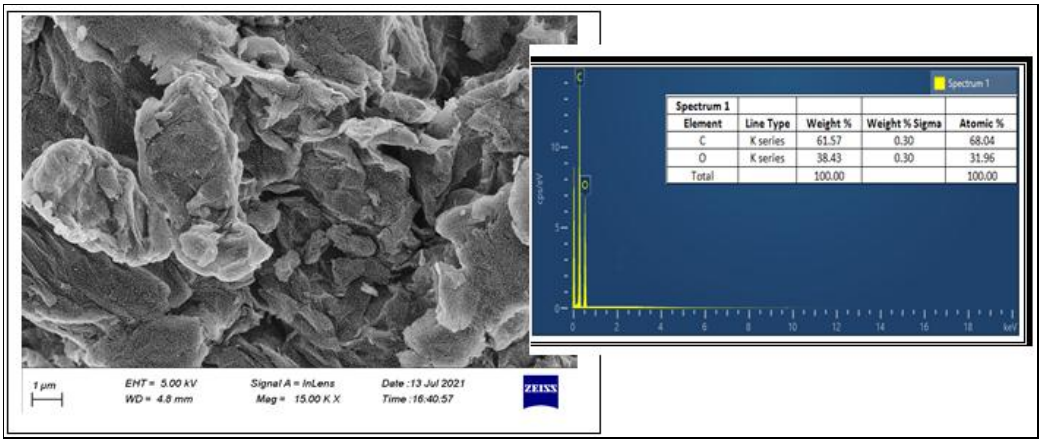

Fig. 4: FESEM Image and EDX of synthesized nano sheets of (GO)

Optimization of solid phase micro extraction method (SPME)

The divalent ions (Mg^{+2}, Co^{+2}, Ni^{+2}, Cu^{+2}, Cd^{+2}, and Pb^{+2}) were carried out using nano sheets of graphene oxide in this study, and the recovery requirement for the SPME method solution was examined spectroscopy of flame atomic absorption (FAAS). The recovery was estimated using the formula R percent = $[(C_{added} - C_{after})/C_{added}]100\%$, where C_{added} represent the direct concentration of the analyte and C_{after} is the analyte concentration as determined by the SMPE method [23]. The ideal pH for (Ni^{+2}, Mg^{+2}, Cd^{+2}, Co^{+2}, Cu^{+2}, and Pb^{+2}, respectively) are 5.5,6.0,.6.5,7.0,7.5, and 8.0, which is sufficient for the chemical adsorption process for each analyte ion on surface area of NGO, When raised the pH, the recovery percentage improves [24] as shown in Fig. (5-a) . Fig. (5-b) shows the recovery of (NGO) mass rose from 0.25 to 1.0 mg, indicating the presence of extra sorption sites on (GO) surface nano sheets [23].

The results reveal that recovery of the analyte ions remained constant between 20 and 50 mL of sample volume, but that metal ion recovery fell below 20 mL, because adsorption capacity is independent on the sample volume under ideal conditions [25] as shown in Fig. (5-c), stirring time (5-120 min) has no effect on the SPME method's results as shown in Fig. (5-d) , The equilibrium reached the accessible sorption sites for metal ions quite soon, indicating that the adsorption process is relatively quick, because the solution was not diffused (accumulated), This resulted in incomplete adsorption on surface NGO, the sonication duration remained consistent in the range (2-10 min), without sonication, the metal ion recovery time was less than 2 minutes as shown in Fig.(5-e).At high temperatures, weak electrostatic attraction interactions exist between metal ions and the surfaces charge of NGO, the recovery of metal ions did not change greatly with temperature, but it did decrease at $70C^0$ (exothermic adsorption) [26] as shown in Fig. (5-f). As indicated in Fig. 1, adsorption efficiency improved considerably as NaCl concentration increased (2 - 6.5 mg mL^{-1}) and declined as NaCl concentration increased (7-8 mg mL^{-1}). Low NaCl concentration (5 g) caused inefficient (GO) agglomeration nano sheets and poor analyte adsorption efficiency, because of the conflict higher NaCl concentrations resulted in significant analyte elution from NGO due to the competitive interactions between the positive sodium

ions and analyte ions [27].Due to competing adsorption between interfering ions and analyte ions, interfering ions may affect analyte adsorption efficiency. The recovery of the measured analyte ions in solutions containing interfering metal ions was assessed The recovery value before and after the interfering metal ions were added, compared with tolerance limits set at the highest ion concentrations that result in fewer than 5% of recovery values [23] as shown in Table 2.

Table. 2: Tolerance limit of interfering ions on the analytes

	Mg^{+2}	Co^{+2}	Ni^{+2}	Cu^{+2}	Cd^{+2}	Pb^{+2}
Cr (III) (µg/mL)	0.8	0.8	0.4	0.8	0.6	0.8
Mn (IV) (µg/mL)	1.0	0.8	0.4	0.8	0.4	1.0
Fe (II) (µg/mL)	5.0	3.0	4.0	5.0	5.0	5.0
Fe (III) (µg/mL)	3.0	2.0	3.0	4.0	3.0	4.0
Zn (II) (µg/mL)	5.0	4.0	2.0	4.0	1.0	3.0
As (III) (µg/mL)	0.8	0.4	0.4	1.0	0.4	0.6
Sn (II) (µg/mL)	0.8	0.8	0.4	0.8	0.6	0.6
Li (I) (µg/mL)	1.0	4.0	3.0	3.0	2.0	4.0
K (I) (µg/mL)	10	40	20	40	40	40
Ca (II) (µg/mL)	10	30	35	26	15	30
Ba (II) (µg/mL)	40	80	80	80	80	80

Adsorption capacity

Analyte adsorption capacity determinate by, $q\ (\mu g/mg) = \frac{(C_o - C)V}{W}$ equation, where q denotes the quantity of analyte adsorbed per unit weight of (GO), (C_o and C) denote the initial and residual analyte concentrations, (V) sample volume, and (W) the weight of (NGO) [25]. Table 3 shows the adsorption capacity of Mg^{+2}, Co^{+2}, Ni^{+2}, Cu^{+2}, Cd^{+2}, and Pb^{+2} (1g/mL) computed at the optimum conditions of the SPME method.

Table 3: Adsorption Capacity of analyte ions (1ug/mL) onto NGO surfaces

Analyte	Recovery%	Adsorption Capacity (µg/mg)
Mg^{+2}	85.1	34.04
Co^{+2}	85.1	34.04
Ni^{+2}	82.2	32.88
Cu^{+2}	71.9	28.76
Cd^{+2}	83.3	33.32
Pb^{+2}	84.9	33.96

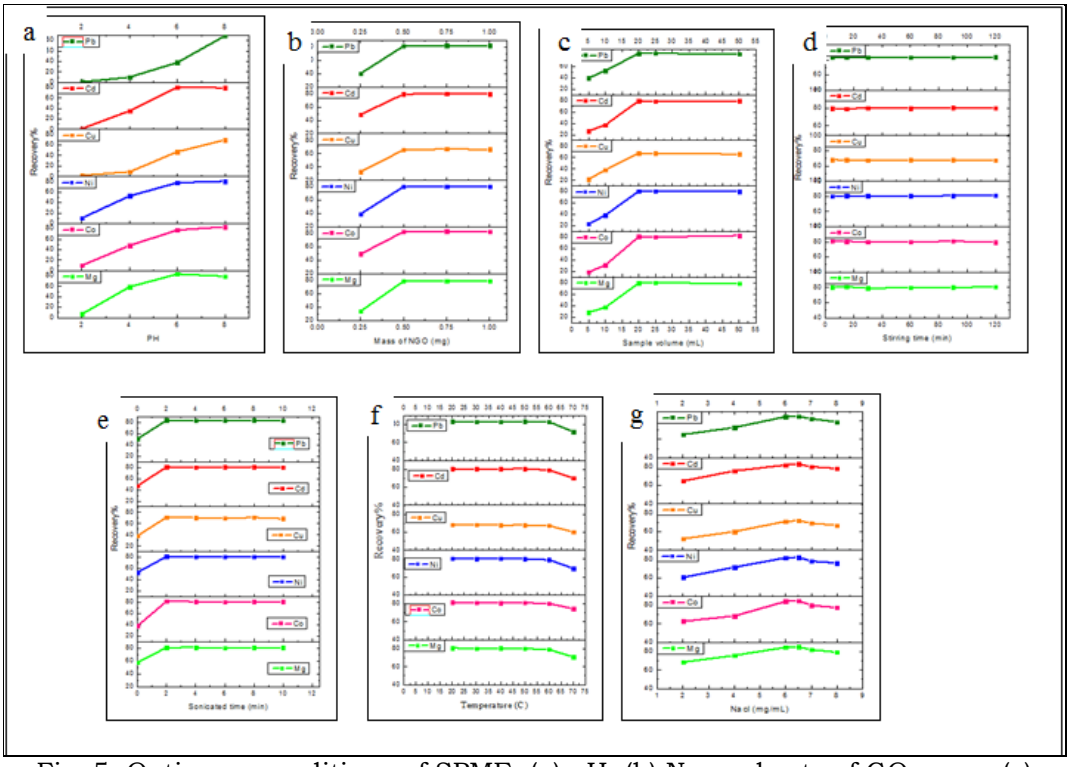

Fig. 5: Optimum conditions of SPME, (a) pH, (b) Nano sheets of GO mass, (c) Sample volume, (d) Stirring time, (e) Sonicated time, (f) Temperature, (g) NaCl Concentration

Analytical performance

Table 4 and Fig. 5 shows the determination of the analyte ions by the direct method with FAAS and using the SPME method under optimum conditions. Magnesium concentrations by using the direct method (9.205, 9.342, 9.649, 9.859, and 10.545 g/mL) in cutting rock samples from the following oil fields: south Buzurgan, Halfayah, Noor, north Buzurgan, and Amarah. Cobalt concentrations in cutting rock samples in the following oil fields: south Buzurgan, north Buzurgan, Halfayah, Noor, and Amarah, as measured by the direct method (1.262, 1.271, 1.307, 1.371, and 1.38 g/mL). Nickel concentrations in cutting rock samples in the following oil fields: Halfayah, Noor, south Buzurgan, north Buzurgan, and Amarah, as determined by the direct method (4.292, 4.464, 5.636, 6.727, and 7.113 g/mL). Copper concentrations in cutting rock samples in the following oil fields: south Buzurgan, north Buzurgan, Amarah, Halfayah, and Noor, as determined by the direct method (0.181, 0.46, 0.51, 0.621, and 1.31 g/mL). Cadmium contents in cutting rock samples in the following oil fields: Halfayah, Noor, Amarah, north Buzurgan, and south Buzurgan were determined using the direct method (0.419, 0.522, 0.548, 0.636, and 0.71 g/mL, respectively). Cutting rock samples from the following oil fields: Amarah, Halfayah, north Buzurgan, south Buzurgan, and Noor were tested for lead amounts using the direct method (2.508, 3.095, 4.38, 5.166, and 31.333 g/mL). Magnesium concentrations in cutting rock samples in the following oil fields:

Buzurgan south area, Halfayah, Noor, Buzurgan north region, and Amarah, as determined by the SPME method (1.842, 1.944, 2.093, 2.169, and 2.364 g/mL). Cobalt concentrations in cutting rock samples in the following oil fields: Halfayah, north Buzurgan, Noor, south Buzurgan, and Amarah, as determined by the SPME method (0.222, 0.238, 0.239, 0.245, and 0.254 g/mL). Nickel concentrations in cutting rock samples in the following oil fields: Halfayah, Noor, south Buzurgan, north Buzurgan, and Amarah, as determined by the SPME method (0.73, 0.785, 1.037, 1.298, and 1.48 g/mL). Copper concentrations in cutting rock samples in the following oil fields: south Buzurgan, north Buzurgan, Amarah, Halfayah, and Noor, as determined by the SPME method (0.047, 0.101, 0.134, 0.16, and 0.369 g/mL). Cadmium concentrations in cutting rock samples at the following oil fields: Halfayah, Noor, Amarah, north Buzurgan, and south Buzurgan, as determined by the SPME method (0.011, 0.035, 0.058, 0.081, and 0.091 g/mL). Cutting rock samples from the oil fields of Amarah, Halfayah, north Buzurgan, south Buzurgan, and Noor were tested for lead concentrations using the SPME method (0.434, 0.557, 0.71, 0.858, and 8.205 g/mL, respectively).

Because of the electrostatic interaction with the NGO surfaces, the concentration of analytes in cutting rock samples decreased utilizing the SPME method. Magnesium recovery percentages in cutting rock samples in the following oil fields: Amarah, north Buzurgan, Noor, Halfayah, and south Buzurgan, correspondingly (77.6 percent, 78.3 percent, 79.2 percent, and 80 percent). Cobalt recovery percentages in cutting rock samples in the following oil fields: south Buzurgan, north Buzurgan, Amarah, Noor, and Halfayah were 80.6 percent, 81.3 percent, 81.6 percent, 82.6 percent, and 83 percent, respectively. In the cutting rock samples from the following oil fields: Amarah, north Buzurgan, south Buzurgan, Noor, and Halfayah, nickel recovery percentages were 79.2 percent, 80.7 percent, 81.6 percent, 82.4 percent, and 83 percent. In the cutting rock samples from the following oil fields: Noor, south Buzurgan, Amarah, Halfayah, and north Buzurgan, copper recovery percentages were 71.8 percent, 73.7 percent, 73.7 percent, 74.2 percent, and 78.3 percent, respectively. Cadmium recovery percentages in cutting rock samples (87.2 percent, 87.3 percent, 89.4 percent, 93.3 percent, and 97.4 percent) at the following oil fields: south Buzurgan, north Buzurgan Amarah, Noor, and Halfayah, respectively. In cutting rock samples from the following oil fields: Noor, Halfayah, Amarah, south Buzurgan, and north Buzurgan, respectively, lead recovery percentages were 73.8 percent, 82 percent, 82.7 percent, 83.4 percent, and 83.8 percent.

The average recovery percent of the analyte ions Cu, Mg, Pb, Ni, Co, and Cd increased gradually (74.3 percent, 78.6 percent, 81.14 percent, 81.4 percent, 81.82 percent, and 90.9 percent) in cutting rock samples, the recovery percent of the analyte ions (71.9 percent, 82.2 percent, 83.3 percent, 84.9 percent, 85.1 percent, and 85.1 percent) of the analytes (1 g/1 μg/mL)

Table 4: The concentration of analytes by direct, SPME methods and recovery in cutting rock samples

Oil field	Analyte																	
	Mg			Co			Ni			Cu			Cd			Pb		
	µg/mL		Recovery %	µg/mL		Recovery %	µg/mL		Recovery %	µg/mL		Recovery %	µg/mL		Recovery %	µg/mL		Recovery %
	Direct method	SPME method		Direct method	SPME method		Direct method	SPME method		Direct method	SPME method		Direct method	SPME method		Direct method	SPME method	
Halfayah (n=5)	9.342	1.944	79.2	1.307	0.2222	83	4.292	0.73	83	0.621	0.16	74.2	0.419	0.011	97.4	3.095	0.557	82
Noor (n=5)	9.649	2.093	78.3	1.371	0.2386	82.6	4.464	0.785	82.4	1.31	0.369	71.8	0.522	0.035	93.3	31.333	8.205	73.8
Amarah (n=5)	10.545	2.364	77.6	1.38	0.2539	81.6	7.113	1.48	79.2	0.51	0.134	73.7	0.548	0.058	89.4	2.508	0.434	82.7
North Buzurgan (n=5)	9.859	2.169	78	1.271	0.2377	81.3	6.727	1.298	80.7	0.46	0.101	78.3	0.636	0.081	87.3	4.38	0.71	83.8
South Buzurgan (n=5)	9.205	1.842	80	1.262	0.2448	80.6	5.636	1.037	81.6	0.181	0.047	73.7	0.71	0.091	87.2	5.166	0.858	83.4
SD±	0.5275	0.2024	0.97	0.055	0.0116	0.976	1.2798	0.3232	1.49	0.4203	0.1231	2.4	0.1112	0.0329	4.38	12.3631	3.387	4.16
RDS %	5.4271	9.7194	1.23	4.1756	4.8534	1.193	22.665	30.322	1.84	68.179	75.874	3.22	19.62	59.513	4.82	132.988	157.33	5.127
Average	9.72	2.0824	78.6	1.3182	0.2394	81.82	5.6464	1.066	81.4	0.6164	0.1622	74.3	0.567	0.0552	90.9	9.2964	2.1528	81.14

* Note: n = 5 (number of samples)
SD ±: standard deviation, RSD%: relative standard deviation

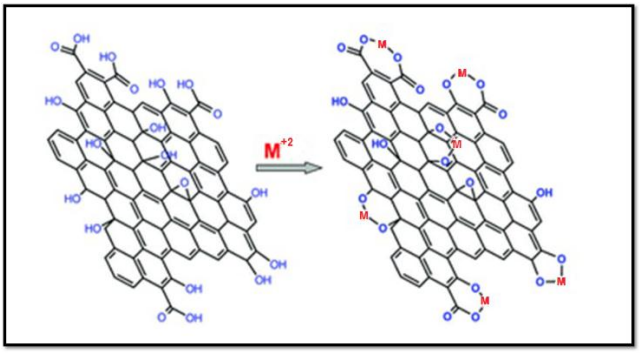

Fig.-6 The mechanism of analyte ions adsorption on nano sheets of (GO)

Conclusion

Graphene oxide was synthesized from graphite oxidation, which was analyzed using several techniques. After the ionization of hydrogen ions of the (-COOH) and (-OH) groups, the anionic groups will attract the cationic analyte ions by electrostatic attraction forces, and epoxy (COC), as shown in Fig.-6. The analyte ions (cation nature) at the optimal pH for each analyte ion, can be adsorbed quickly and efficiently on NGO sheet surfaces. The adsorption process including, temperature, pH, contact time, adsorbent dosage, and metal ion starting concentration are very important parameters. In analyte ion adsorption affinity on (NGO) surfaces, electronegativity, initial stability constant, and standard reduction potential all play a role, with standard reduction potentials of (-2.37 v) and (+0.34 v) for Mg^{+2} and Cu^{+2} ions, respectively, with Mg^{+2} having a higher recovery percent than Cu^{+2}. However, depending on whether the heat of

adsorption is exothermic or endothermic, Temperature has the ability to increase or decrease the capacity. Increasing the temperature increases however, It lowers the specific adsorption capacity while raising the adsorption rate and metal ion removal percentage. Furthermore, increasing the solid mass content may cause the (NGO) to fold, preventing access to the active binding sites. Longer contact periods ensure that equilibrium and maximal adsorption capacity are achieved under those precise conditions. The charge of the (NGO) and the ion species in the solution are affected by the pH of the solution. Cationic ion exchange chromatography is the proposed method, in which (GO) nano sheets (anionic nature) serve as a stationary phase sorbent and analyte solution (cationic nature) serves as a mobile phase sorbent. This approach has the benefit of being inexpensive, time efficient, and economical, as it uses only 0.5mg NGO as a sorbent. SPME is a new technology for separating metal ions from cutting rock samples after they have been cut. The interfering ions has no substantial effect on analyte recovery and adsorption efficiency, the suggested method can be used to analyze materials with high salt concentration.

Acknowledgment

The authors are grateful for the laboratory facilities provided by the Department of Chemistry, College of Science, University of Misan.

References

1. Srogi K. *Developments in the Determination of Trace Elements by Atomic Spectroscopic Techniques*. Vol 41.; 2008.
2. Wang Y, Gao S, Zang X, Li J, Ma J. Graphene-based solid-phase extraction combined with flame atomic absorption spectrometry for a sensitive determination of trace amounts of lead in environmental water and vegetable samples. *Anal Chim Acta*. 2012;716:112-118.
3. Zhang L, Hu X, Zhu L, Jin X, Feng C. Water-dispersible ZnO/COFe2O4/graphene photocatalyst and their high-performance in water treatment. *Fullerenes Nanotub Carbon Nanostructures*. 2019;27(11):873-877.
4. Lin S, Shih CJ, Strano MS, Blankschtein D. Molecular insights into the surface morphology, layering structure, and aggregation kinetics of surfactant-stabilized graphene dispersions. *J Am Chem Soc*. 2011;133(32):12810-12823.
5. An X, Simmons T, Shah R, et al. Stable aqueous dispersions of noncovalently functionalized graphene from graphite and their multifunctional high-performance applications. *Nano Lett*. 2010;10(11):4295-4301.
6. Ibrahim F, Bakir ET, Ali SM. Synthesis of Nickel Ferrite NiFe 2 O 4 Nanoparticles / PVA composite and studying Its electric properties. *Tikrit J Pure Sci*. 2016;21(6):55-60.
7. Su S, Chen B, He M, Hu B, Xiao Z. Determination of trace/ultratrace rare earth elements in environmental samples by ICP-MS after magnetic solid phase extraction with Fe_3O_4@SiO_2@polyaniline-graphene oxide composite. *Talanta*. 2014;119:458-466.
8. Kudin KN, Ozbas B, Schniepp HC, Prud'homme RK, Aksay IA, Car R. Raman spectra of graphite oxide and functionalized graphene sheets. *Nano Lett*. 2008;8(1):36-41.

9. Zhao G, Ren X, Gao X, et al. Removal of Pb(ii) ions from aqueous solutions on few-layered graphene oxide nanosheets. *Dalt Trans*. 2011;40(41):10945-10952.
10. Mcallister MJ, Li J, Adamson DH, et al. Expansion of Graphite. *Society*. 2007;19(4):4396-4404.
11. Chen J, Yao B, Li C, Shi G. An improved Hummers method for eco-friendly synthesis of graphene oxide. *Carbon N Y*. 2013;64(1):225-229.
12. Zaaba NI, Foo KL, Hashim U, Tan SJ, Liu WW, Voon CH. Synthesis of Graphene Oxide using Modified Hummers Method: Solvent Influence. *Procedia Eng*. 2017;184:469-477.
13. Tsolakidou A, Buxeda I Garrigós J, Kilikoglou V. Assessment of dissolution techniques for the analysis of ceramic samples by plasma spectrometry. *Anal Chim Acta*. 2002;474(1-2):177-188.
14. Hu Z, Qi L. Sample Digestion Methods. *Treatise Geochemistry Second Ed*. 2013;15(January 2014):87-109.
15. Crouch S, Skoog D, Holler FJ. *Principles of Instrumental Analysis Seventh Edition*. Vol 88.; 2016.
16. Varenne F, Coty JB, Botton J, et al. Evaluation of zeta potential of nanomaterials by electrophoretic light scattering: Fast field reversal versus Slow field reversal modes. *Talanta*. 2019;205(June):120062.
17. Ain QT, Haq SH, Alshammari A, Al-Mutlaq MA, Anjum MN. The systemic effect of PEG-nGO-induced oxidative stress in vivo in a rodent model. *Beilstein J Nanotechnol*. 2019;10(April):901-911.
18. Stobinski L, Lesiak B, Malolepszy A, et al. Graphene oxide and reduced graphene oxide studied by the XRD, TEM and electron spectroscopy methods. *J Electron Spectros Relat Phenomena*. 2014;195(March 2018):145-154.
19. Krishnamoorthy K, Veerapandian M, Yun K, Kim SJ. The chemical and structural analysis of graphene oxide with different degrees of oxidation. *Carbon N Y*. 2013;53:38-49.
20. Drewniak S, Muzyka R, Stolarczyk A, Pustelny T, Kotyczka-Morańska M, Setkiewicz M. Studies of reduced graphene oxide and graphite oxide in the aspect of their possible application in gas sensors. *Sensors (Switzerland)*. 2016;16(1).
21. Zaaba NI, Foo KL, Hashim U, Tan SJ, Liu WW, Voon CH. Synthesis of Graphene Oxide using Modified Hummers Method: Solvent Influence. *Procedia Eng*. 2017;184:469-477.
22. Xu Y, Nguyen Q, Malekahmadi O, et al. Synthesis and characterization of additive graphene oxide nanoparticles dispersed in water: Experimental and theoretical viscosity prediction of non-Newtonian nanofluid. *Math Methods Appl Sci*. 2020;(February):1-20.
23. Beata Zawisza, Rafal Sitko EM and ET. Graphene oxide as a solid sorbent for the preconcentration of cobalt, nickel, copper, zinc and lead prior to determination by energydispersive X-ray fluorescence spectrometry. *Anal Methods*. 2013;3(1):2-6.
24. Wu W, Yang Y, Zhou H, et al. Highly efficient removal of Cu(II) from aqueous solution by using graphene oxide. *Water Air Soil Pollut*. 2013;224(1).
25. Liou TH, Lin MH. Characterization of graphene oxide supported porous silica for effectively enhancing adsorption of dyes. *Sep Sci Technol*. 2020;55(3):431-443.
26. Atkins, P. W.; de Paula J. Physical Chemistry (8th ed.). *Oxford Univ Press*.

Published online 2006:764.
27. Deng D, Jiang X, Yang L, Hou X, Zheng C. Organic solvent-free cloud point extraction-like methodology using aggregation of graphene oxide. *Anal Chem*. 2014;86(1):758-765.